



Comparative analysis of mechanical properties of scaffolds sintered from Ti and Ti6Al4V powders

L. A. Dobrzański ^a, A. D. Dobrzańska-Danikiewicz ^a, A. Achtelek-Franczak ^{a,*},
L. B. Dobrzański ^b

^a Faculty of Mechanical Engineering, Silesian University of Technology, ul. Konarskiego 18a,
44-100 Gliwice, Poland

^b Center of Medicine and Dentistry Sobieski, Jana III Sobieskiego 12/1, 44-100 Gliwice, Poland

* Corresponding e-mail address: anna.achtelek-franczak@polsl.pl

ABSTRACT

Purpose: The aim of the article is to present and compare the results of studies into mechanical properties, including mainly tensile and compressive strength of scaffolds fabricated from Ti and Ti6Al4V in Selective Laser Sintering (SLS) for specific sintering conditions.

Design/methodology/approach: Titanium scaffolds characterised by the different size of pores were fabricated on the basis of 3D CAD models of samples for tensile and compressive strength examinations prepared with AutoFab software for a selected unit cell. The so prepared samples were subject to tensile and compressive strength examinations with a universal tensile testing machine Zwick 020.

Findings: The results of examinations of mechanical properties of pristine titanium and its alloy Ti6Al4 showing differences in the strength of the two materials and allowing to characterise each of them. The size of pores and the shape and manner of arrangement of a unit cell building the scaffold influences substantially the strength properties of titanium scaffolds.

Practical implications: The scaffolds with specific strength properties fabricated in the SLS process create conditions for their application in dental engineering and in jaw-face reconstructions.

Originality/value: The original results of tensile and compressive strength examinations of the created scaffolds. The innovative application of the rapid manufacturing technology for the purpose of regenerative medicine may greatly influence the development of this field of medicine.

Keywords: Biomaterials; Titanium and Ti6Al4V scaffolds; Selective laser sintering; Tensile strength; Compressive strength

Reference to this paper should be given in the following way:

L.A. Dobrzański, A.D. Dobrzańska-Danikiewicz, A. Achtelek-Franczak, L.B. Dobrzański, Comparative analysis of mechanical properties of scaffolds sintered from Ti and Ti6Al4V powders, Archives of Materials Science and Engineering 73/2 (2015) 69-81.

PROPERTIES

1. Introduction

Rapid manufacturing technologies are becoming more and more widespread and popular across various industries these days. Their advantages allow to develop multiple disciplines in the field of engineering wherever a clear need exists for producing elements with a complicated shape, geometry and a distinctive structure. RM technologies are based on 3D CAD models, on the basis of which a specific element is manufactured using a given technology. RM technologies, by combining the phase of design during which a model is created with customised properties, with the manufacturing phase, have become highly competitive vis-à-vis the numerous traditional manufacturing technologies used to date, including casting or machining. Numerous diverse rapid manufacturing technologies are used in industry these days, which may differ in the type and form of the materials used, a combination method of particular material layers, as well as construction possibilities; these are always computer-controlled technologies, though, requiring the earlier preparation of appropriate 3D CAD models of the object produced [1-3].

2. Porous materials in medicine

Porous structures are very desired in medicine, especially where a porous element is to replace a missing bone. In such situation, the task of the element produced is to stimulate a regeneration process of the adjacent bone tissue. Titanium scaffolds fabricated with SLS technologies should be characterised by the appropriate size of pores, appropriate porosity, as well as the strength permitting usage in dental engineering as bone implants functioning as scaffolds, which become a substructure and support for the bone growing into them. Literature data shows [4-15] that the size of pores allowing the development of the bone growth process into the created scaffold varies between the minimum of 50-200 μm and the maximum of 500 μm , and the porosity of such scaffold should exceed 50%. A satisfactory result of a manufacturing process of porous titanium materials is seen when an element is achieved with open pores, characterised by an appropriate level of porosity and sufficiently good strength properties.

Bone porosity is referred to as the volume fraction of the fluid phase filling the pore space of a bone in a given bone volume unit. The bone fluid phase consists of blood vessels, nerve fibres, bone cells and extracellular bone fluid. A cortical bone has the density of 1.99 g/cm^3 . It has the longitudinal compressive strength of 131-224 MPa and

the longitudinal bending strength of 79-151 MPa. The transverse compressive strength of a cortical bone is 106-133 MPa, and bending strength is 51-56 MPa [16-17].

Technologies employing space fillers are currently the very popular fabrication methods of titanium materials. In such technologies, titanium powder and another powder representing a pore filler with a specific size of particles are mixed. After mixing the powder, the shape of the object created is formed by cold or hot pressing, die pressing or injection moulding. The object created is then subjected to additional treatment, e.g. machining, as material density is often increased in moulding at the material - mould/die boundary, leading to the closing of pores. The additional treatment applied allows to open the pores and to transfer a moulding to another phase in which a filler is removed. The filler can be removed by various processes, including: (i) thermolysis; (ii) burning and removing the burnt filler with a stream of inert gas; (iii) filler solving in liquid. The removed filler leaves pores, and the so produced material undergoes a vacuum sintering process. The technologies applying a space filler enable to fabricate materials with specific porosity, size of pores and strength, as characterised in Table 1 with reference to the data presented in the publications established by different research teams [13-15, 18-22].

The disadvantages of these technologies is a need to apply dies or moulds and, considering a small production scale of implants, it leads to very high production costs. It is also problematic to acquire implants free of contaminants, such as oxide, nitride, carbon, which very often accompany a fabrication process of porous implants using the space filler technology. When using dies or moulds, the elements forming part of them may entrain the element being produced, thus creating numerous contaminants which are very hard to remove from the final product. An issue of the complicated geometry of implants and the presence of contaminants in the final product is solved by RM technologies, where a fabrication process is carried out in a chamber filled with inert gas and takes place without using any dies or moulds.

Due to the advantages of RM technologies and the opportunities they bring, they have become very popular in medicine, where they are employed mainly for manufacturing: (i) physical models of anatomical organs for training and educational purposes, as well as models used in operative treatment for operation planning; (ii) surgical instruments; (iii) dental and orthodontic models; (iv) dental implants and bridges; (v) customised implants adjusted to the patient based on the results of computer tomography examinations, magnetic nuclear magnetic resonance or traditional plaster casts.

Table 1.
The properties of porous materials manufactured with space fillers

Porosity [%]	Pore size [μm]	Strength [MPa]	References
45-70	~500	15-116	[13,18]
45-75	70-400	24-168	[14,15]
55-80	200-300	1,5-30	[19]
60-80	200-500	10-35	[20-22]

The issue of reconstructing the damaged bone tissues has been known for long and affects many patients nowadays. Bone loss replacement using the appropriate material to restore the original function is undertaken by numerous specialist studies led in engineering, medical and dental sciences, as well as by interdisciplinary studies being at the interface of such disciplines. A very important aspect addressed by patients are aesthetic considerations, as well, relating in particular to symmetry by restoring an anatomical shape of the lost bone and restoring the satisfactory appearance. The issues presented above are being resolved in various ways by selection of an appropriate material and technique for producing a part of the lost bone. At present, natural or synthetic materials are used optionally in regenerative surgery and implantology in substantiated cases. The following groups of materials are distinguished for materials of the natural origin used in this area: (i) autogenous bones taken from a patient's bone; (ii) alloplastic bones mentioned when a graft comes from one donor of the same species; (iii) xenogeneic bones most often of the animal origin. The following groups of basic materials are classified as the key alloplastic materials of the synthetic origin: (i) ceramics, e.g. hydroxyapatite, aluminium oxide, zirconium oxide, bioglass; (ii) polymers, e.g. polymethyl methacrylate (PMMA); (iii) metals, e.g. titanium, titanium alloys, chromium-cobalt alloys, surgical steel and composites created by combining at least two materials belonging to the above-mentioned basic groups.

The material expected to replace a missing bone should have the following characteristics [23-30]:

- appropriate biocompatibility characterised by the lack of allergic and cytotoxic reactions in contact with living tissues,
- biological safety signifying that full sterility and asepsis can be ensured,
- resorption and substitution ability similar to the bone,
- the resorption or degradation level of tissue synchronised with bone restoration,
- an ability to fill the space of the loss,

- appropriate mechanical stabilisation,
- appropriate porosity of the materials produced,
- an osteoconductive activity connected with osteoconductivity being a process of bone loss regeneration consisting of the in-growth of vessels called osteoblasts into the grafting material, which are bone forming cells originating from the adjoining bone stock,
- an osteoinductive activity where the differentiation of mesenchymal cells is stimulated in the environment of osteoblasts, by assuming that mesenchyme is the connective embryonal tissue occurring only in the embryonic period, from which all types of connective tissues, bone tissue, cartilage tissue and muscle tissue are created.

Therefore, rapid manufacturing enables to create objects with the ultimate shape while allowing to control the fabricated element in each part of its volume. An advantage of RM technologies is also an ability to fabricate without applying costly and time intensive casting moulds, as a result of which the product obtained does not contain external admixtures which often occur in the cast products. The maximum possible reduction of wastes generated in a manufacturing process as compared to waste-generating machining ranks RM technologies higher than the traditional manufacturing processes applied until now. The entire rapid manufacturing process is taking place in an atmosphere of inert gas, which prevents the creation of unwanted products of the reactions occurring between a material used for fabrication of elements and air components.

3. Materials and methodology

A material used for tests is pristine titanium (grade 2) and Ti6Al4V titanium alloy (grade 23) with the chemical composition consistent with the manufacturer's specification shown in Table 2.

Titanium is considered a light metal with the density of $\rho = 4,507 \text{ g/cm}^3$, the melting point of 1668°C and boiling point of 3260°C . It occurs in two allotropic variants, i.e. α and β . The α titanium variant has a hexagonal lattice (A3), which, at the temperature of 882.5°C , is transformed into a high-temperature variant β crystallising in the cubic system (A2). Due to its properties such as high mechanical strength relative to the mass and high corrosion resistance, titanium has been broadly used in the military, aviation, space and chemical sector and in medicine [18,31,32].

Table 2.
Chemical composition of powders used for experiments expressed in mass per cents [36-37]

Powder	Al	V	C	O	N	H	Fe	others everyone	others together	Ti
Ti	–	–	0.01	0.14	0.01	0.004	0.03	<0.01	<0.4	rest
Ti6Al4V	6.5	4.1	0.01	0.08	0.01	0.0019	0.17	<0.01	<0.4	rest

Titanium's essential properties allowing to employ it in medicine including high biocompatibility with living tissues and pitting corrosion resistance, intercrystalline corrosion resistance and stress corrosion resistance. Pristine titanium occurs in the single-phase variant α , and titanium alloy Ti6Al4V in the double-phase variant α and β [18,31,32]. Titanium and titanium alloys are at present the most popular materials used in implantation treatment. Implants made of ready parts such as titanium plate or rods are mainly available at the market. Such parts undergo mechanical treatment as a result of which a final product is obtained suitable for implantation. Commercial titanium implants, so-called titanium plates, are fabricated in several shapes. For this reason, a surgeon must adjust the shape of the implant to the bone loss during a surgical procedure. The selective laser sintering (SLS) technology permits to fabricate an implant with a specific shape and thickness, adjusted to specific needs of a patient.

The powders used in an SLS process, namely: titanium and Ti6Al4V, apart from suitable purity and the grain size of up to 45 μm , also have lower oxygen contents of, respectively, 0.14% and 0.08%, so that the process can be carried out safely while the standard average oxygen content in titanium powders is about 0.5%. Excessive oxygen content could lead to its sudden reactions with titanium and to explosion. An oxygen concentration in a sintering process of titanium or its biomedical alloys should not exceed 50 ppm, while this value for steels is much higher and should not exceed 1000 ppm.

All the samples for strength tests were made with the AM device by Renishaw for selective laser sintering. The time needed to design an object depends on its size, structure complexity, as well as the number of elements which are made in a given process at a time. The fabrication accuracy of objects depends on the laser power applied. For example, for the layer thickness of 20 to 50 μm , it is ± 20 μm in the XY plane for low laser power and ± 100 μm for high laser power. The device is also integrated with suitable software allowing to accommodate the designed model to the fabrication process conditions. The process of selective laser sintering

can be divided into two phases. In the first phase a given element is designed and the result is a 3D CAD model recorded in a file with *stl* extension. This format allows to present a model with a lattice of triangles, and the smaller the triangles the more accurate surface representation. The following is done subsequently in the first phase in particular: (i) an element is divided into layers with particular thickness; (ii) optimum fabrication process conditions are established, such as: laser power, scanning speed, layer thickness, distance between remelting paths, laser beam diameter; (iii) the model designed is transferred to machine software. The second phase comprises the actual fabrication process for selective sintering with laser of an element designed in prior by means of a computer, which takes place after achieving a vacuum and a protective atmosphere in the device.

A database of unit cells incorporated in AutoFab software [33,34] was used for fabricating titanium scaffolds by SWLS technology. Unit cells differing in the shape and wall thickness are provided in the AutoFab database, which allows to create, through the multiplication of units cells, scaffolds with a different geometric shape.

Scaffold models are created using a previously selected unit cell with a hexagonal structure (Fig. 1). In the place where individual arms are joined, a hexagonal cell has characteristic strengthening which may be very meaningful for strengthening the entire scaffold structure, thus enhancing the strength properties of the object created. A manner of arrangement of a unit cell in the space of a system of coordinates also influences the strength properties. In order to identify how the unit cell arrangement method in the entire scaffold structure influences the strength properties, CAD models of scaffolds were created with the following unit cell arrangement in the space of a system of coordinates:

- a unit cell is arranged in the plane of a system of coordinates (Fig. 2a),
- a unit cell is rotated in respect of the axis x of the system of coordinates by 45° (Fig. 2b),
- a unit cell is rotated in respect of the axis y of the system of coordinates by 45° (Fig. 2c).

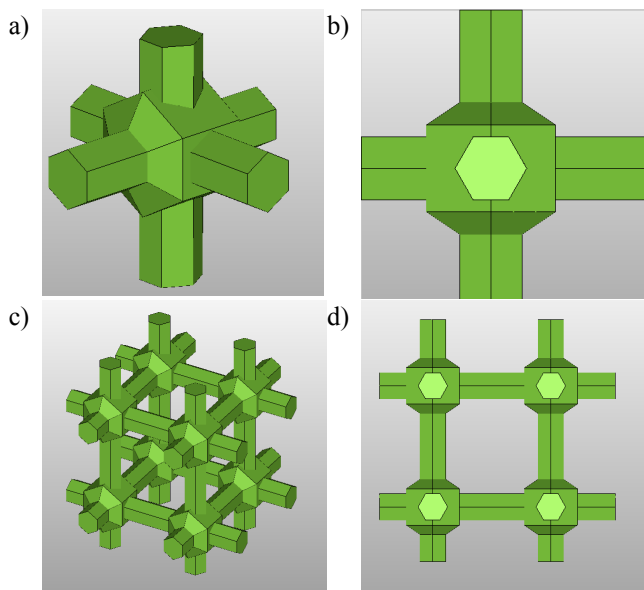


Fig. 1. Hexagonal unit shape: a) a single unit cell; b) top view of single unit cell; c) scaffold part composed of eight unit cells; d) top view of scaffold part reflecting the shape of its pores

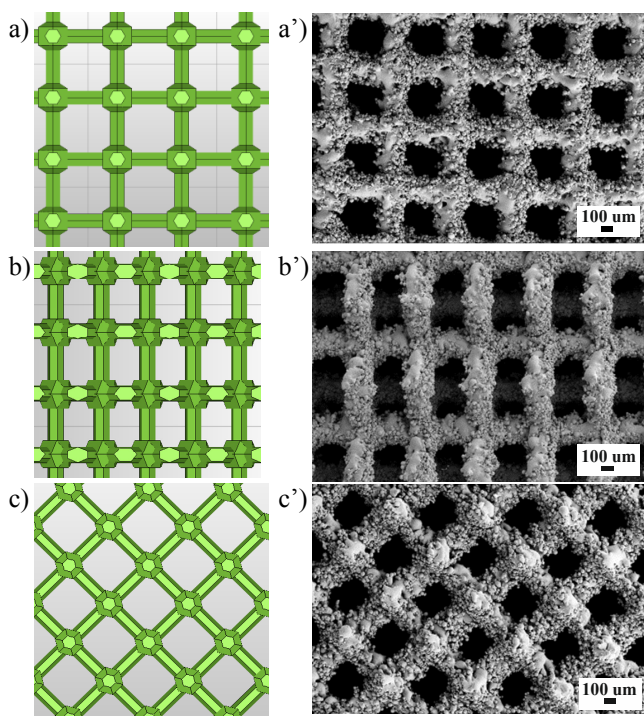


Fig. 2. The porous structure of a scaffold with a different arrangement of a unit cell in the space of a system of coordinates; a)-c) CAD models; a')-c') SEM images

Next, the particular 3D models designed with AutoFab software were transformed into a net of triangles, by recording them in the *stl* format and after transferring the data into the device, the actual objects were created, as shown in Fig. 2a')-c').

Scaffolds sintered with a laser selectively with the AM device by Renishaw were subjected to microscope examinations with a Scanning Electron Microscope SEM Supra 35 by Carl Zeiss equipped with an Energy Dispersive Spectroscopy (EDS) by EDAX. The mechanical properties of the newly created scaffolds were examined with a tensile testing machine ZWICK/Roell Z100.

4. Scaffolds tensile strength

The porous titanium materials fabricated by selective laser sintering were underwent tensile strength tests. Results for the maximum tensile strength of F_m were obtained as a result of tensile strength tests, and a tensile strength value was calculated accordingly with the formula (1) corresponding to tensile strength [35].

$$R_m = \frac{F_m}{S_0} \left[\frac{N}{\text{mm}^2} = \text{MPa} \right] \quad (1)$$

where:

F_m - maximum compressive force;

S_0 - field area of cross section of sample;

R_m - tensile strength.

The sample models for tensile strength tests are presented in Fig. 3. Five samples were made for each of three different unit cell arrangements in the space of the system of coordinates (Fig. 3b,c,d). Two types of hexagonal unit cells inscribed into a cube with the side length of, respectively, 600 μm and 500 μm , were designed in order to perform tensile strength tests. The average size of pores for the material consisting of unit cells with the side of 600 μm is 350 μm , as shown in Fig. 4. The size of pores corresponding to a porous structure of material consisting of multiplied unit cells inscribing into a cube with the size of 500 μm is smaller and on average is 250 μm (Fig. 5).

The averaged results of the maximum compressive force F_m recorded in the tests and of the tensile strength value R_m calculated according to the formula (1), are presented in Table 3. The table also presents porosity values of the scaffolds produced, calculated on the basis of the volume of the samples produced and their density, by

reference the density of solid material. A table with results of the studies indicate that the dimensions of the pores achieved as well as the porosity of the titanium materials fabricated by SLS are within the range beneficial and desired for materials used in medicine, which should exhibit osteoconductive properties.

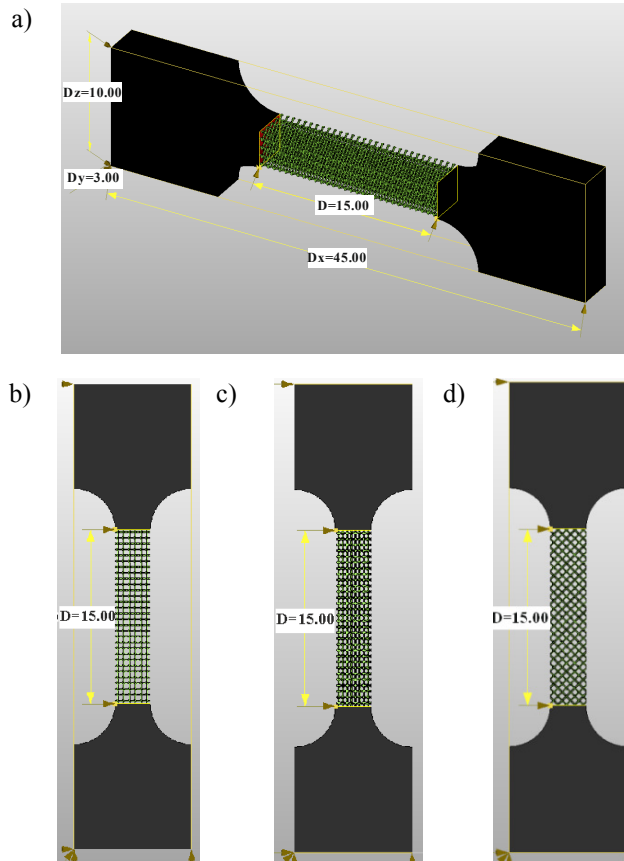


Fig. 3. Samples for tensile strength tests; 3D model with sample dimensions provided (a); views corresponding to the unit cell arrangement: in the plane of the system of coordinates (b) of the system of coordinates (c) under the angle of 45° relative to the axis x (d) and axis y

Table 3.

Results of tensile strength tests for porous titanium made for samples with different arrangement of unit cell relative to the axis of system of coordinates

Unit cell arrangement	Size of pores S_0 [mm ²]	350 μ m			250 μ m		
		F_m [N]	R_m [MPa]	Porosity [%]	F_m [N]	R_m [MPa]	Porosity [%]
0°	9	91.47	10.16	74.45	105.78	11.75	66.63
45°x	9	106.94	11.88	74.87	168.68	18.74	67.27
45°y	9	86.37	9.60	75.29	97.52	10.83	67.86

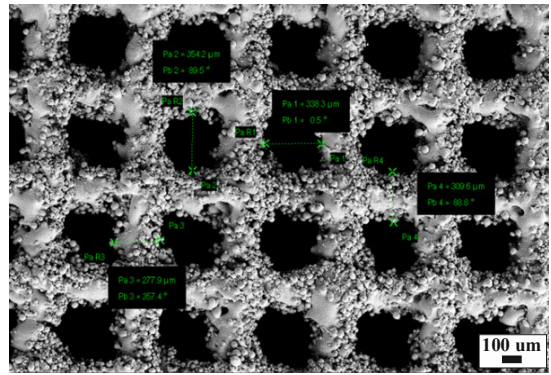


Fig. 4. SEM image of titanium porous material consisting of multiplied unit cells with the side of 600 μ m

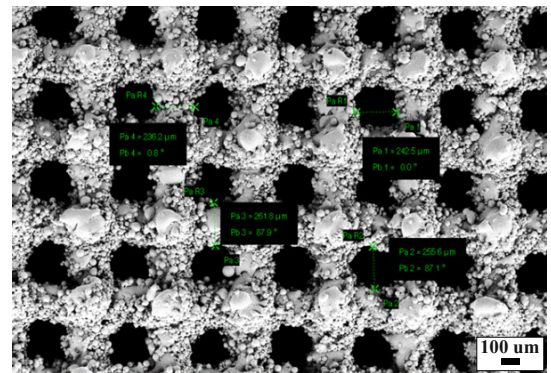


Fig. 5. SEM image of structure of titanium porous material consisting of multiplied unit cells with the side of 500 μ m

Figure 6 shows a dependency of elongation, expressed in per cents, from the tensile strength value determined for titanium scaffolds produced for different unit cell arrangement in the space of the system of coordinates. The highest tensile strength value was achieved for the unit cell arranged at the angle of 45° relative to the axis x. A different arrangement of unit cells relative to the axis of the system of coordinates is influencing the different curve of the laser path sintering the powder.

Figure 7 shows laser paths for three consecutive layers for the unit cell arranged in the plane of a system of coordinates (Fig. 7a) at the angle of 45° in relation to the axis x (Fig. 7b) and at the angle of 45° relative to the axis y (Fig. 7c). A dependency can be observed - while analysing the results of the studies - between the strength of particular samples and the uniform arrangement of the curve of the laser acting on the particular layers of the powder being sintered.

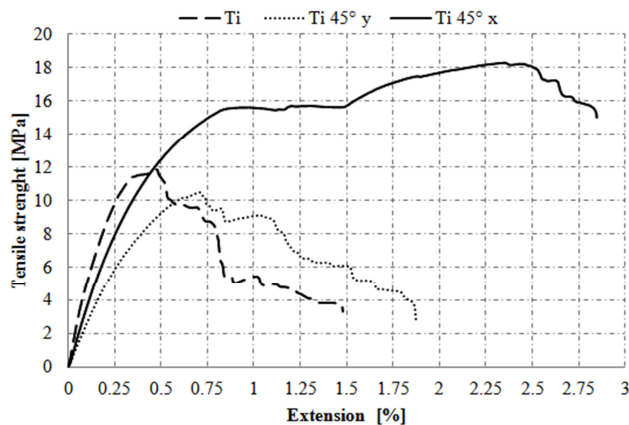


Fig. 6. Charts of dependence between extension and tensile strength for titanium samples produced for the different relative position with regard to the axis of the system of coordinates of a unit cell inscribed into a cube with the side of 500 μm

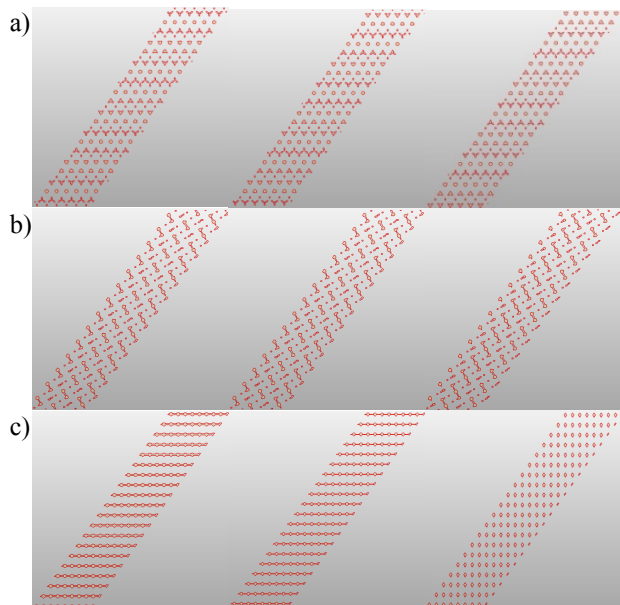


Fig. 7. Path curve of a laser sintering the three particular powder layers for unit cell arranged in the plane of the system of coordinates (a) of the system of coordinates (b) for angle 45° in relation to the axis x (c) and axis y

As seen from Fig. 6, the highest tensile strength values were achieved for a unit cell arranged at the angle of 45° relative to the axis x. It can be concluded by analysing the curve of the laser path for this arrangement that its appearance for particular layers differ insignificantly meaning that the laser is acting uniformly on the particular powder layers when sintering the particular powder layers. Observations also allow to establish that - considering the comparable laser paths - the most homogenous is the path corresponding to the sintering of powder layers for a unit cell arranged at the angle of 45° in relation to the axis x. The smallest tensile strength is exhibited by the samples where until cells are arranged at the angle of 45° relative to the axis y. Laser paths in this case for particular layers differ substantially, causing the laser to be acting non-uniformly on a given layer of powder, which influences the weakening of the entire scaffold structure.

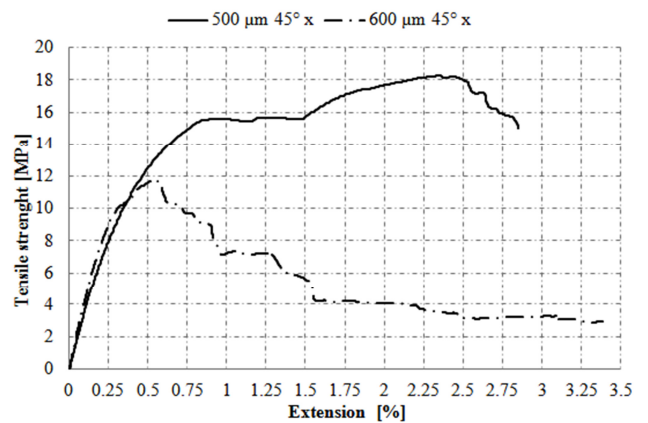


Fig. 8. Chart of dependence between elongation and tensile strength for unit cells inscribed into a cube with the side of 500 and 600 μm arranged at the angle of 45° relative to the axis x

It can be noticed by analysing a chart presented in Fig. 6 that for a sample with the unit cells arranged at the angle of 45° relative to the axis x, a clear yield strength R_e exists for the tensile strength of 15.5 MPa. Sample elongation is clearly increasing for such a strength value, by reaching about 0.8%. Yield strength for other samples is not so noticeable though, and is not noticeable at all, sometimes. Sample elongation occurring under the influence of tensile strength is also conditional upon the size of scaffold pores. It was noticed that tensile strength is increasing as the size of pores is decreasing, as presented in Figure 8.

Tensile strength tests of titanium scaffolds with the different arrangement of a unit cell relative to the axis of the system of coordinates (Fig. 6) and with varied porosity (Fig. 8) were carried out by using the standard laser path curve settings recommended by the manufacturer, called the

path I by the authors of the article. A laser path curve was changed during experiments, and the path, by contrast, was called the path II, which has influenced the change of the structure and has improved the strength properties of the elements produced. The field area of the cross section of the scaffolds fabricated with the path I is shown in Fig. 9, while Fig. 10 presents a fracture of a sample produced using the path II. While improving the precision of laser interaction on the particular powder layers, by applying the path II, the actual structure of the scaffold was greatly improved, which became more uniform and cohesive, which is manifested by a smaller number of voids observed in the fracture in relation to a fracture of the scaffold produced for the standard laser path progress setting. If the path II is employed, the powder is sintered accurately and precisely due to the activity of a laser on the powder and a material flow effect is achieved, which is observed at high magnification (500 x), as waves formed in one direction, and the path of laser interaction with the powder is clearly visible. A structure of a titanium scaffold manufactured with the standard path I is similar at

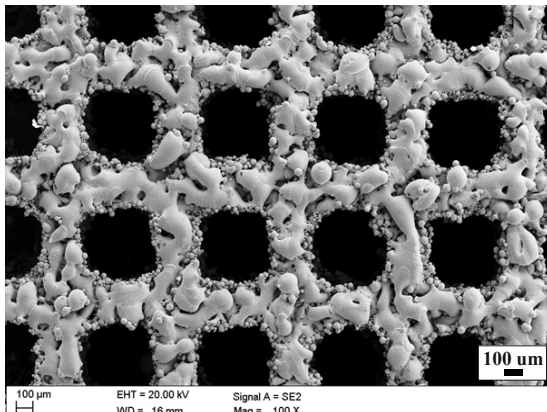


Fig. 9. Scaffold fracture manufactured with the path I of laser curve

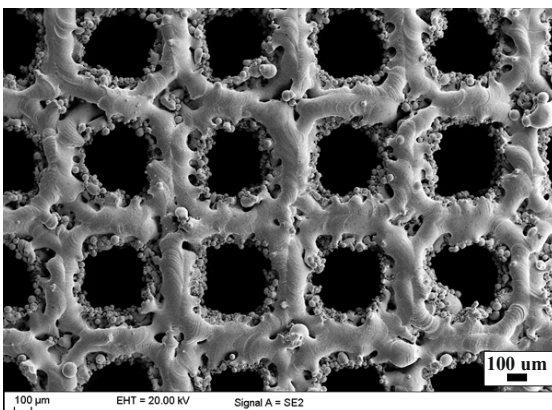


Fig. 10. Scaffold fracture manufactured with the path II of laser curve

the fracture to a disordered jigsaw consisting of pieces of sintered powder loosely connected with each other and forming the sort of a mosaic.

Figure 11 presents dependency charts of material elongation and tensile strength created for titanium scaffolds with, respectively, the path I and path II of a laser curve. A comparative analysis undertaken indicates that improved laser-to-powder activity precision through changes to the laser path curve settings contributes to greatly improved material tensile strength. A two-fold improvement is seen for this strength, by growing from 18 MPa, registered for a scaffold fabricated with the path I of a laser curve, to 35 MPa achieved in the case of a scaffold fabricated with the path II.

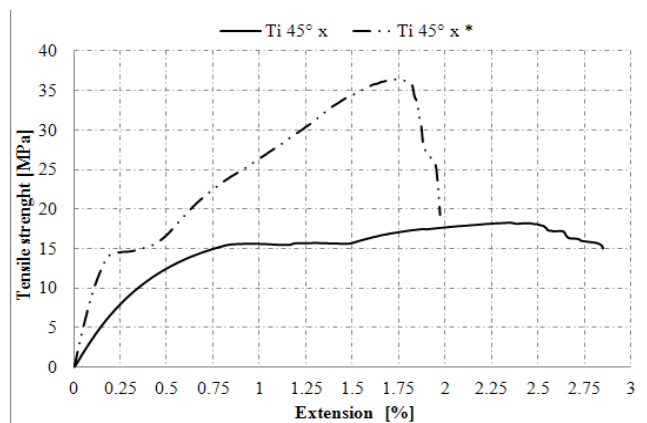


Fig. 11 Chart of dependence between extension and tensile strength for titanium scaffolds consisting of unit cells with the side of 500 μm arranged at the angle of 45° relative to the axis x manufactured with the path I and path II (symbol: *) of laser curve

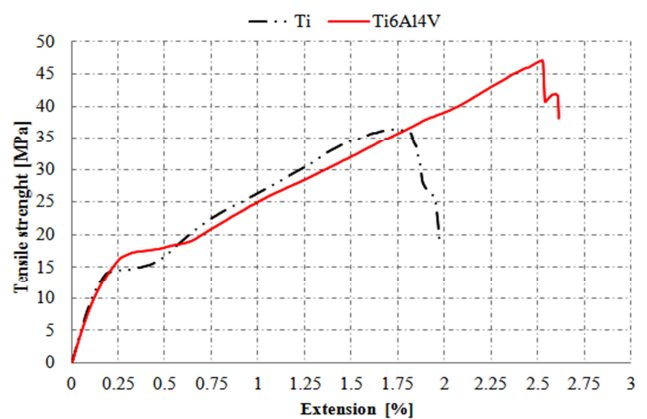


Fig. 12. Chart of dependence between extension and tensile strength for titanium scaffolds and scaffolds made of Ti6Al4V alloy consisting of unit cells with the side of 500 μm arranged at the angle of 45° relative to the axis x manufactured with the path II of laser curve

A series of experiments was carried out, by replacing the titanium powder used so far with Ti6Al4V powder, after selecting the optimum size of scaffold pores and the best unit cell arrangement relative to the axis of the system of coordinates and after selecting an optimum laser curve path. The average tensile strength of the laser-sintered material made of Ti6Al4V titanium alloy determined according to five tests is 47.15 MPa and is 30% higher than a value corresponding to a scaffold manufactured in identical conditions with titanium powder. The comparative charts for scaffolds made of titanium and Ti6Al4V allow are shown in Figure 12. The characteristic of tensile progression curves proves that both, the porous titanium as well as porous Ti6Al4V titanium alloy are elastic-plastic materials with a clearly marked elastic strength and yield strength.

5. Scaffolds compressive strength

Compressive strength corresponding to compressive strength was calculated using maximum compressive force according to formula (2) [35].

$$R_c = \frac{F_m}{S_0} \left[\frac{N}{\text{mm}^2} = \text{MPa} \right] \quad (2)$$

where:

R_c - compressive strength;

F_m - maximum compressive force;

S_0 - field area of the original cross section of the sample.

Two types of hexagonal samples consisting of multiplied hexagonal unit cells inscribed into a cube with the side length of, respectively, 600 μm and 500 μm , were designed in order to perform compressive strength tests. The average size of pores in the scaffolds fabricated this way for unit cells with the side of 600 μm is 350 μm , and for a unit cell with the size of 500 μm it is accordingly smaller and is 250 μm . Samples for compressive strength tests (Fig. 13), similar as samples for tensile strength tests, were fabricated for three different unit cell arrangements in

relation to the axis of the system of coordinates. Five samples were made for each of the arrangements. The averaged results of the maximum compressive force F_m recorded during the tests and of the tensile strength value R_m calculated according to the formula (2) are presented in Table 4. The detailed results of the examinations into the dependency between the material deformation and compressive strength are also presented graphically in a series of charts (Figs 14-17).

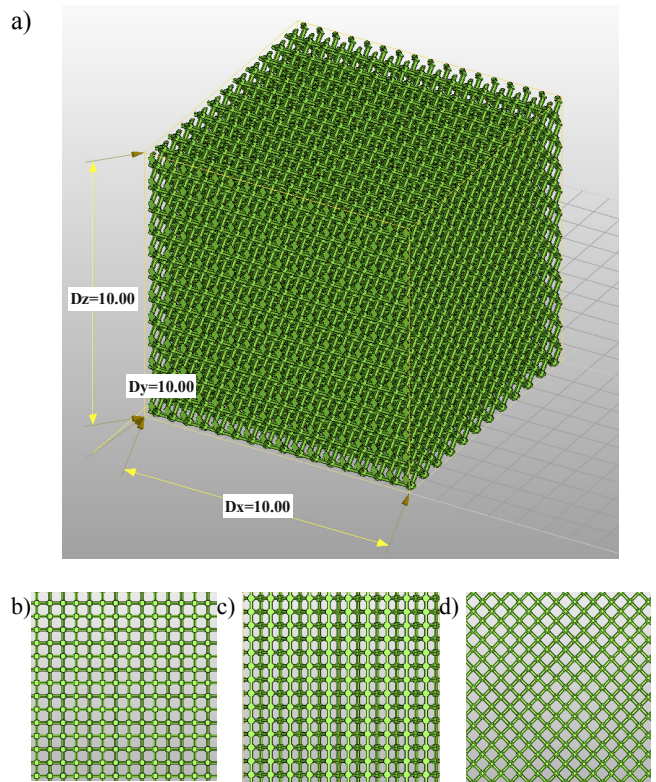


Fig 13. Samples for compressive strength tests; 3D model with sample dimensions provided (a); views corresponding to the unit cell arrangement: in the plane of the system of coordinates (b) of the system of coordinates (c) under the angle of 45° relative to the axis x (d) and axis y

Table 4.

Results of compressive strength tests for porous titanium made for samples with different arrangement of unit cell relative to the axis of system of coordinates

Size of pores	350 μm			250 μm		
Unit cell arrangement	S_0 [mm^2]	F_m [N]	R_c [MPa]	F_m [N]	R_c [MPa]	
0°	141.42	5118.63	36.19	7107.80	50.26	
45°x	141.42	3814.62	26.97	5334.13	37.71	
45°y	141.42	1224.69	8.66	1963.27	13.83	

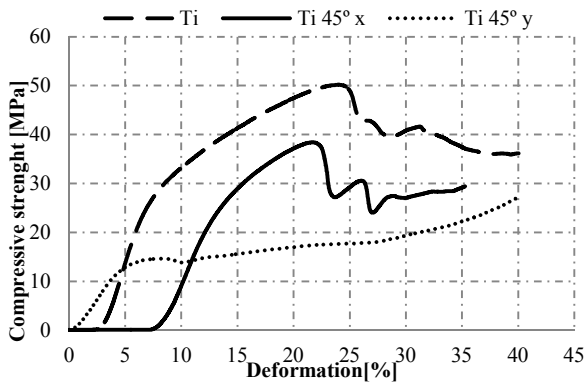


Fig. 14 Chart of dependence between deformation and compressive strength for titanium samples produced for the different relative position with regard to the axis of the system of coordinates of a unit cell inscribed into a cube with the side of 500 μm

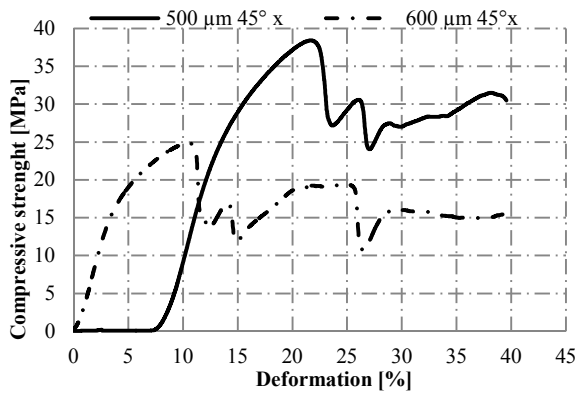


Fig. 15. Charts of dependence between deformation and compressive strength for unit cells inscribed into a cube with the side of 500 and 600 μm arranged at the angle of 45° relative to the axis

It was pointed out by analysing the experimental data obtained that the highest values of the maximum compressive force F_c , on the basis of which values were calculated of the compressive strength corresponding to compressive force, were attained for scaffolds made up of unit cells with the side of 500 μm arranged in the plane of the system of coordinates. The second highest compressive strength values were recorded for scaffolds comprised of unit cells arranged at the angle of 45° relative to the axis x, which saw the best tensile strength tests results. The scaffolds created by sintering the unit cells arranged at the angle of 45° relative to the axis y possess the lower compressive strength as signified by the lowest values of the compressive strength recorded. The results obtained are

another evidence that there is a clear correlation between the strength of particular samples and the uniform influence of the laser path on the particular layers of the sintered powder. Comparative charts for compressive strength tests were carried out, similar as in the case of tensile strength tests, for scaffolds consisting of unit cells arranged at the angle of 45° relative to the axis x.

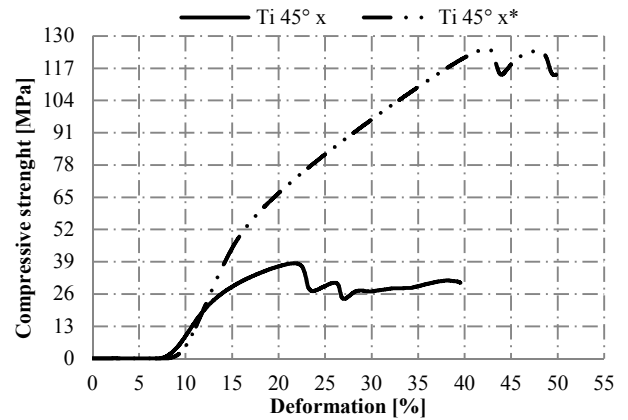


Fig. 16. Chart of dependence between deformation and compressive strength for titanium scaffolds consisting of unit cells with the side of 500 μm arranged at the angle of 45° relative to the axis x manufactured with the path I and path II (symbol: *) of laser curve

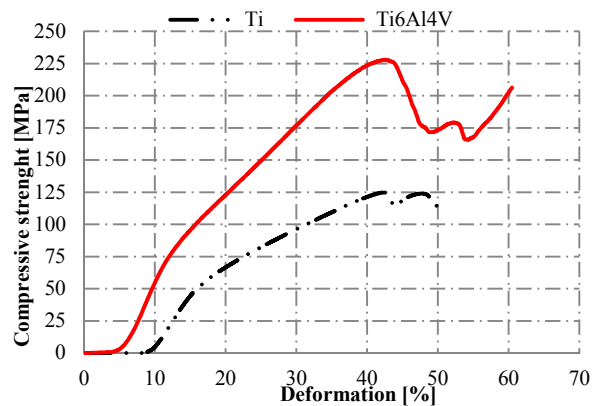


Fig. 17. Chart of dependence between deformation and tensile strength for titanium scaffolds and scaffolds made of Ti6Al4V alloy consisting of unit cells with the side of 500 μm arranged at the angle of 45° relative to the axis x manufactured with the path II of laser curve

In the case where material is being compressed with the high porosity of 65-75%, its deformation is very high and reaches over 20% for the maximum compressive force

value. Such large deformations stem from the fact that particular scaffold latticework layers are folding like a fan under the influence of compressive force. In connection with the above, in the curves of the charts corresponding to scaffolds consisting of unit cells arranged in the plane of the system of coordinates and at the angle of 45° relative to the axis x, distinctive blisters similar to mountain peaks are observed. The compressive strength, when reaching a local maximum, leads to the rupture of the particular scaffold spans, and is then decreased until the next scaffold spans are met, when it rises again. The sequence is repeated several times during one test.

Samples for compressive strength tests, similar as samples for tensile strength tests, have been produced using the standard path I of laser curve (Figs 14 and 15), and the path II (Fig. 16) ensuring a more uniform and cohesive scaffold structure. The tensile strength of the scaffolds fabricated with the path II of laser progression reaches the value of over 120 MPa and is twice better as compared to the scaffolds produced with the path I.

Similar as in the case of tensile strength tests, for the pre-defined optimum process conditions, samples were also fabricated for compressive strength tests using Ti6Al4V titanium alloy powders for this purpose. The average compressive strength value of over 225 MPa was achieved after performing compressive strength tests for a series of five samples. This means that a scaffold made of Ti6Al4V titanium alloy has compressive strength higher by 87% as compared to a scaffold made of pristine titanium, as shown in Figure 17.

6. Conclusions

The selective laser sintering technology allows to shapen the mechanical properties of the fabricated porous titanium materials by using multiple factors which can be controlled in many directions and which can be deliberately selected to achieve synergy. The factors include not only quite obvious conditions of a manufacturing process such as: laser power, laser point diameter, powder layer thickness, distance between particular remelting paths, but also factors which are selected well in advance, already at the stage of process design using specialist computer tools for this purpose. This group of factors shapening a structure and mechanical properties of porous materials and materials analysed in this article include: shape of a unit cell building the porous material, the size of this cell and the resulting size of scaffold pores, unit cell arrangement with regard to the system of coordinates as well as a path

curve of a laser sintering the particular powder layers. All the experiments performed also show that if a relatively small amount of Al (6% by mass) and V (4% by mass) of titanium powder is added, a two-fold increase in mechanical properties of the scaffolds fabricated in identical conditions is achieved.

The results obtained for examinations into strength properties can be compared to the strength of porous materials fabricated with other methods. For example, the strength of the porous materials manufactured with space fillers may be up to about 168 MPa for porosity of ca. 40%. The SLS technology can be employed for producing materials with porosity of up to 80% and the strength of up to 125 MPa for titanium and even up to 225 MPa for Ti6Al4V titanium alloy. It should also be underlined that the advantage of rapid manufacturing technologies distinguishing them from other manufacturing technologies of porous materials include not only the lack of possibility to contaminate the final product with other materials applied in the fabrication process, but also a possibility to fully control the shape and size of the pores achieved. SLS also ensures nearly waste-free production.

Acknowledgements

The works have been implemented within the framework of the BIOLASIN project entitled "Investigations of structure and properties of newly created porous biomimetic materials fabricated by selective laser sintering" headed by Prof. L.A. Dobrzański, funded by the Polish National Science Centre in the framework of the "Harmony 4" competitions. The project was awarded a subsidy under the decision DEC-2013/08/M/ST8/00818.

Additional information

Selected issues related to this paper are planned to be presented at the 22nd Winter International Scientific Conference on Achievements in Mechanical and Materials Engineering Winter-AMME'2015 in the framework of the Bidisciplinary Occasional Scientific Session BOSS'2015 celebrating the 10th anniversary of the foundation of the Association of Computational Materials Science and Surface Engineering and the World Academy of Materials and Manufacturing Engineering and of the foundation of the Worldwide Journal of Achievements in Materials and Manufacturing Engineering.

References

- [1] L. Lu, J. Fuh, Y. Wong, *Laser Indused Materials and Processes for Rapid Prototyping*, Kluwer Publishers, Dordrecht, 2001.
- [2] S. Kumar, *Selective Laser Sintering: A Qualitative and Objective Approach, Modeling and Characterization* (2003) 43-47.
- [3] M. Miecielica, *Rapid Prototyping Technologies*, PM 2 (2010) 39-45.
- [4] M. Klimek, *The use of SLS technology in making permanent dental restorations*, *Prosthetics* 12 (2012) 47-55 (in Polish).
- [5] L.S. Bertol, W.K. Júnior, F.P. da Silva, C.A. Kopp, *Medical design: Direct metal laser sintering of Ti-6Al-4V*, *Materials and Design* 31 (2010) 3982-3988.
- [6] L. Ciocca, M. Fantini, F. De Crescenzo, G. Corinaldesi, R. Scott, *Direct metal laser sintering (DMLS) of a customized titanium mesh for prosthetically guided bone regeneration of atrophic maxillary arches*, *Medical and Biological Engineering and Computing* 49 (2011) 1347-1352.
- [7] P.A. Mazzoli, *Selective laser sintering in biomedical engineering*, *Medical & Biological Engineering and Computing* 51 (2013) 245-256.
- [8] A. Bandyopadhyay, F. Espana, V.K. Balla, S. Bose, Y. Ohgami, N.M. Davies, *Influence of porosity on mechanical properties and in vivo response of Ti6Al4V implants*, *Acta Biomaterialia* 6 (2010) 1640-1648.
- [9] S. Van Bael, Y.C. Chai, S. Truscetto, et al., *The effect of pore geometry on the in vitro biological behavior of human periosteum-derived cells seeded on selective laser-melted Ti6Al4V bone scaffolds*, *Acta Biomaterialia* 8/7 (2012) 2824-2834.
- [10] I.V. Shishkovsky, V. Scherbakov, *Selective laser sintering of biopolymers with micro and nano ceramic additives for medicine* *Physics Procedia* 39 (2012) 491-499.
- [11] L.A. Dobrzański, *Overview and general ideas of the development of constructions, materials, technologies and clinical applications of scaffolds engineering for regenerative medicine*, *Archives of Materials Science and Engineering* 69/2 (2014) 53-80.
- [12] R. Melechow, K. Tubielewicz, W. Błaszczak, *Titanium and its alloys: types, properties, applications, treatment technology, degradation*, PC Press, Częstochowa, 2004 (in Polish).
- [13] L.A. Dobrzański, *Fundamentals of materials science*, Silesian University of Technology Press, Gliwice, 2012 (in Polish).
- [14] L.A. Dobrzański, *Descriptive metallurgy of non-ferrous metal alloys*, Wydawnictwo Politechniki Śląskiej, Gliwice, 2009 (in Polish).
- [15] A. Nouri, P.D. Hodgson, C. Wen, *Biomimetic Porous Titanium Scaffolds for Orthopedic and Dental Applications*, *Biomimetics, Learning from Nature*, Australia (2010) 415-450.
- [16] S.W. Kim, H.D. Jung, M.H. Kang, H.E. Kim, Y.H. Koh, Y. Estrin, *Fabrication of porous titanium scaffold with controlled porous structure and net-shape using magnesium as spacer*, *Materials Science and Engineering C* 33/5 (2013) 2808-2815.
- [17] Y. Wang, Y. Shen, Z. Wang, J. Yang, et al, *Development of highly porous titanium scaffolds by selective laser melting*, *Materials Letters* 64 (2010) 674-676.
- [18] G. Ryan, A. Pandit, D.P. Apatsidis, *Fabrication methods of porous metals for use in orthopaedic applications*, *Biomaterials* 27 (2006) 2651-2670.
- [19] S.J. Simske, R.A. Ayers, T.A. Bateman, *Porous materials for bone engineering*, *Materials Science Forum* 250 (1997) 151-182.
- [20] L. M. R. de Vasconcellos, M. V. de Oliveira, M. L. de Alencastro Graça, *Porous Titanium Scaffolds Produced by Powder Metallurgy for Biomedical Applications*, *Materials Research* 11/3 (2008) 275-280.
- [21] Z. Esen, S. Bor, *Processing of titanium foams using magnesium spacer particles*, *Scripta Materialia* 56 (2007) 341-344.
- [22] M. Bram, H. Schiefer, D. Bogdanski, M. Köller, H.P. Buchkremer, D. Stöver, *Implant surgery, How bone bonds to PM titanium?* *Metal Powder Report* 61 (2006) 26-31.
- [23] L.A. Dobrzański, A.D. Dobrzańska-Danikiewicz, P. Malara, T.G. Gaweł, L.B. Dobrzański, A. Achtelik-Franczak, *Selective Laser Sintering and Melting of pristine titanium and titanium Ti6Al4V alloy powders and selection of chemical environment for etching of such materials*, *Archives of Metallurgy and Materials* 60/3 (2015) 2039-2045.
- [24] W. Xue, B.V. Krishna, A. Bandyopadhyay, S. Bose, *Processing and biocompatibility evaluation of laser processed porous titanium*, *Acta Biomaterialia* 3 (2007) 1007-1018.
- [25] M. Bram, C. Stiller, H.P. Buchkremer, D. Stover, H. Baur, *High-porosity titanium, stainless steel, and superalloy parts*, *Advanced Engineering Materials* 2 (2000) 196-199.
- [26] B. Dąbrowski, W. Świeszkowski, D. Godliński, K.J. Kurzydłowski, *Highly porous titanium scaffolds for orthopaedic applications*, *Journal of Biomedical Materials Research B* 95B/1 (2010) 53-61.

- [27] R.C. Thomson, M.C. Wake, M.J. Yaszemski, A.G. Mikos, Biodegradable polymer scaffolds to regenerate organs. *Advances in Polymer Science* 122 (1995) 245-274.
- [28] M. Veiseh, D. Edmondson, Bone as an Open Cell Porous Material, ME 599K: Special Topics in Cellular Solids, 2003.
- [29] A. Laptev, O. Vyal, M. Bram, H.P. Buchkremer, D. Stöver, Green strength of powder compacts provided for production of highly porous titanium parts, *Powder Metallurgy* 48 (2005) 358-364.
- [30] Z. Esen, S. Bor, Processing of titanium foams using magnesium spacer particles, *Scripta Materialia* 56 (2007) 341-344.
- [31] A. Bansiddhi, D.C. Dunand, Shape-memory NiTi foams produced by solid-state replication with NaF. *Intermetallics* 15 (2007) 1612-1622.
- [32] A. Bansiddhi, D.C. Dunand, Shape-memory NiTi foams produced by replication of NaCl space-holders, *Acta Biomaterialia* 4 (2008) 1996-2007.
- [33] L.A. Dobrzański, A. Achtelek-Franczak, M. Król, Computer Aided Design in Selective Laser Sintering (SLS) - application in medicine, *Journal of Achievements in Materials and Manufacturing Engineering* 60/2 (2013) 66-75.
- [34] L.A. Dobrzański, A.D. Dobrzańska-Danikiewicz, et al., Fabrication of scaffolds from Ti6Al4V powders using the computer aided laser method, *Archives of Metallurgy and Materials* 60/2 (2015) 1065-1070.
- [35] L.A. Dobrzański, R. Nowosielski, Test methods of metals and alloys: physical properties studies, WNT Press, Warszawa, 1987.
- [36] Material Safety Data Sheet of CP Titanium, Kamb.
- [37] Material Safety Data Sheet of Ti6Al4V, Kamb.